Available online at www.sciencedirect.com

ScienceDirect

IFAC Papers Online CONFERENCE PAPER ARCHIVE

IFAC PapersOnLine 58-14 (2024) 513–518

Optimal Flexible Operation of Electrified and Heat-Integrated Biodiesel Production

Mohammad El Wajeh, Adel Mhamdi, Alexander Mitsos *

Aachen Process Engineering – Process Systems Engineering, RWTH Aachen University, 52056 Aachen, Germany

* *e-mail: amitsos@alum.mit.edu*

Abstract: We recently investigated the optimal flexible operation of electrified biodiesel production, employing different process configurations with buffer tanks but without heat integration (https://doi.org/10.1021/acs.iecr.3c03074). Herein, we study the implications of incorporating heat integration on process flexibility. We present two process configurations that include heat integration across all three process columns. One of these configurations incorporates additional heating units for reboilers, while the other operates without them. As expected, introducing additional heating units increases process flexibility, yielding higher energy cost savings. We also propose a third configuration wherein we deploy two decentralized optimizers, reducing computational expenses while achieving comparable energy cost savings.

Keywords: Production scheduling, Process optimization, Heat integration, Demand-side management, Process electrification, Optimal control problem

1. INTRODUCTION

The flexible operation of electrified chemical processes, driven by renewable electricity, presents economic and possibly ecological incentives toward a more sustainable chemical industry (Mitsos et al. (2018); Barton (2020)). However, achieving this transformative shift entails a departure from the conventional steady-state (SS) mode of operation, which poses a notable challenge to the fields of process design and operation (Cegla et al. (2023)).

We recently proposed electrifying biodiesel production and investigated its optimal flexible operation using intermediate and final buffer tanks (El Wajeh et al. (2024)). We explored the operational flexibility of three process configurations and compared the outcomes of their dynamic optimization (DO) strategies with those of an optimal SS operation while considering a typical demand-response scenario. Our findings underscored that, as expected, intermediate buffer tanks facilitate the full realization of process flexibility potential, leading to heightened economic performance in dynamic operations. However, this process design did not incorporate heat integration (HI). The integration of heat across multiple units is a prevalent practice in complex and modern chemical plants, aiming for energy efficiency, i.e., minimal external energy supply. Despite this, the optimal flexible operation in heat-integrated chemical processes with the aid of buffer tanks remains underexplored. HI introduces additional intricacies and interdependencies among unit operations, potentially making the flexible operation more intricate and constraining the optimization options (Chen and Yang (2021)).

Herein, we examine how HI impacts the flexible operation of the previously considered biodiesel production process, particularly in terms of the degrees of freedom available for optimization. We present three different process configurations for HI. In the initial two configurations, complete HI is applied to all three distillation columns within the process. We investigate the flexible operation of the process, both with and without external heating units for the reboilers. Since these additional heating units are only relevant in the context of flexible operation, particularly concerning demand-side management, our objective is to assess the effect of these external heat sources on the process flexibility in dynamic operation.

Furthermore, we introduce a third configuration allowing the implementation of two decentralized optimizers, each dealing with a smaller problem. This contrasts with the centralized approach adopted in the other configurations. Within this setup, vapor recompression (VRC) (Harwardt and Marquardt (2012); Guedes do Nascimento et al. (2023)) is applied to one column, while the other two columns are heat-integrated. This configuration stems from the potential demonstrated by decentralized optimizers in terms of computational performance, as highlighted in our prior work (El Wajeh et al. (2024)). The three configurations are subsequently benchmarked against their respective SS operations, as well as against a dynamic operation of a previous configuration without HI. While our evaluation of the three configurations is based on economic objectives, the inclusion of additional units in each configuration may have varying implications for sustainability in terms of overall energy consumption and capital costs.

The structure of the manuscript unfolds as follows. We begin with detailing the configurations employed for HI within the biodiesel production process. Following this, we present the formulation of the solved optimization problems before elaborating on their implementation and the operational scenario considered. Lastly, we present and

10.1016/j.ifacol.2024.08.388

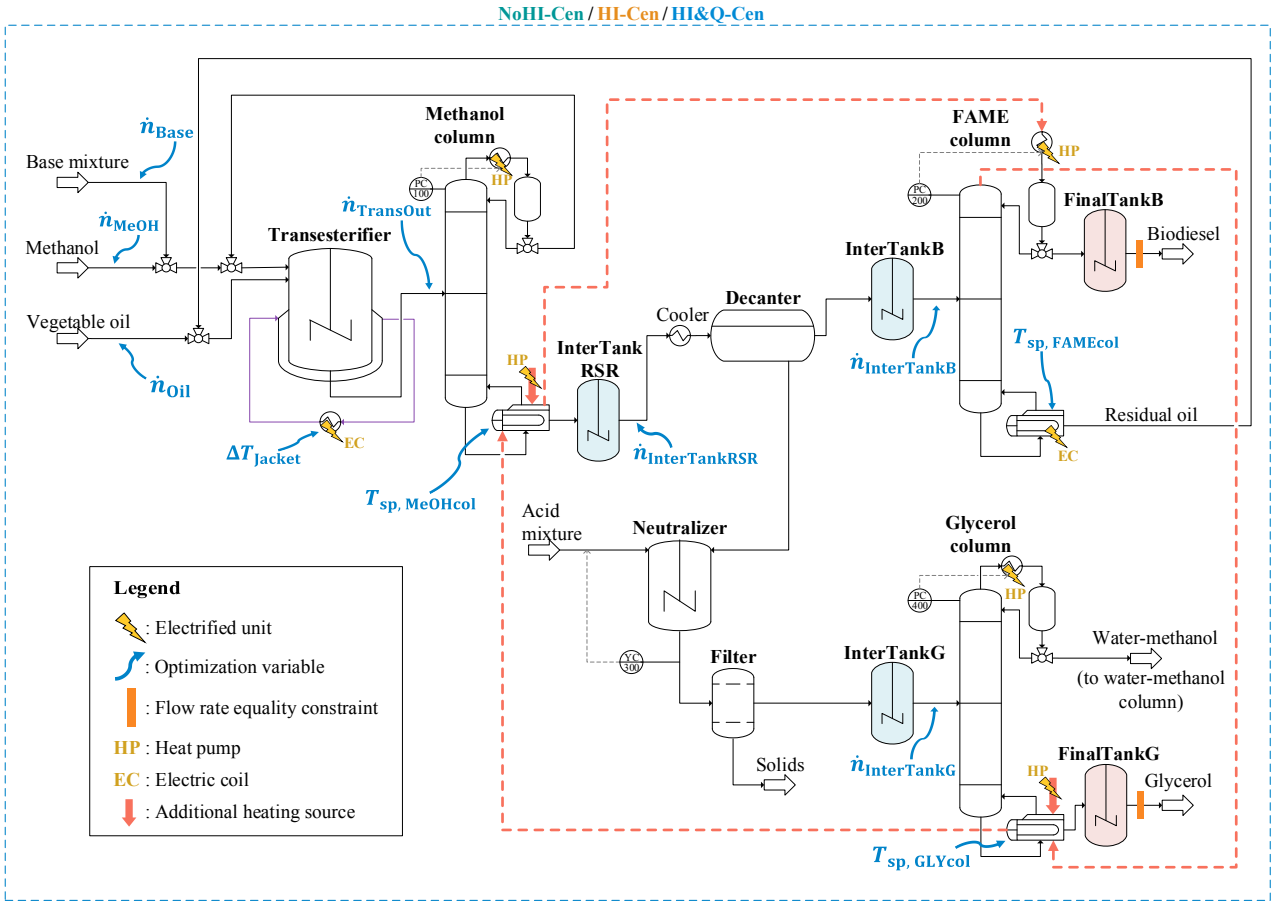

Fig. 1. Biodiesel process flowsheet including both intermediate and final buffer tanks and incorporating a centralized optimization approach. The configurations with full heat integration adopt this flowsheet, wherein the heat-integrated three columns are interconnected by the dashed-red streams depicted.

discuss the findings derived from this study, before drawing our conclusions.

2. BIODIESEL PRODUCTION APPLICATION

In El Wajeh et al. (2023), we introduced and delineated the biodiesel production process under consideration, presenting its dynamic model and making it readily accessible open source. More recently (El Wajeh et al. (2024)), we explored its flexible operation for demand-side management, investigating different process configurations and optimization methodologies. Herein, we use the process configuration that incorporates both intermediate and final buffer tanks and extend it to accommodate HI. Consequently, we focus only on explaining these specific configurations along with their corresponding optimization strategies.

2.1 Process configurations with full heat integration

Fig. 1 illustrates the considered process with full HI across the three distillation columns within the system. The heat exchange in the transesterifier system primarily operates in cooling mode, utilizing room-temperature water, while its electrified heating mode (cf. El Wajeh et al. (2024)), if activated at all, is negligible compared to the power demand of the columns. The transesterifier is thus not considered in the HI. We provide a succinct explanation here regarding the necessity of the buffer tanks depicted, and we direct readers to our prior work (El Wajeh et al. (2024)) for more detailed description.

The potential for flexibility varies among different unit operations, determined not only by their operational limits but also by their locations within the process. To exemplify, limitations on liquid levels in downstream processes can impede the flexibility of production in upstream processes. An effective remedy involves the incorporation of intermediate buffer tanks between distinct sections of the process, enabling the uncoupling of their dynamics and thereby facilitating the maximal utilization of overall production flexibility. In the context of this study, we introduce the buffer tank `InterTankRSR` to fully unlock the production flexibility potential of the methanol column. This is essential as the output production rate of this column is constrained by liquid level limitations in downstream processes, specifically the decanter and columns. Moreover, `InterTankB` and `InterTankG` enable variable production rates within the other downstream power-consuming units, namely the FAME and glycerol columns, respectively. Additionally, `FinalTankB` and `FinalTankG` are indispensable in enabling flexible production of both purities and flow rates while simultaneously fulfilling the demands for final products.

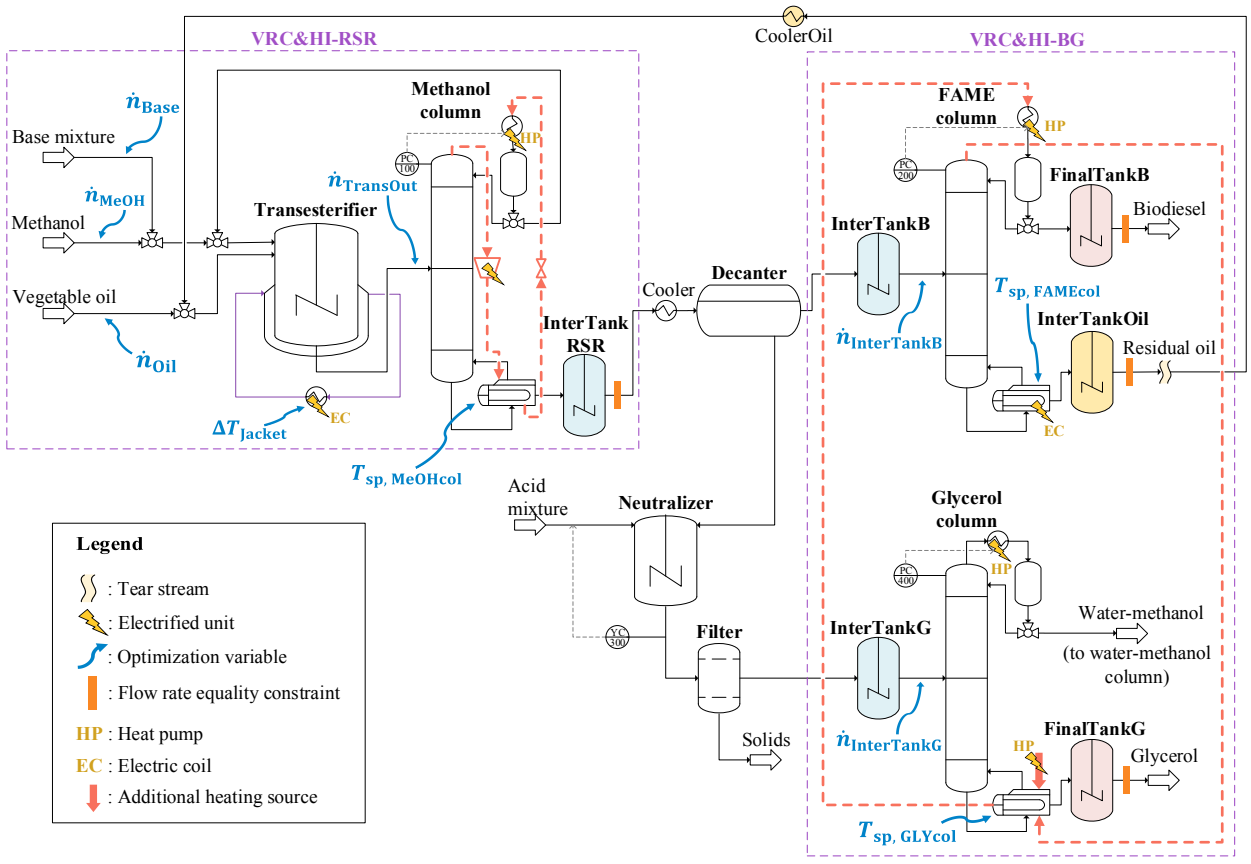

Fig. 2. Biodiesel process flowsheet incorporating intermediate and final buffer tanks and employing a decentralized optimization approach. The configuration with vapor recompression and heat integration adopts this flowsheet. As indicated by dashed-red streams, the methanol column utilizes vapor recompression, while the other two columns are heat-integrated. Two decentralized optimizers are considered here (VRC&HI-RSR and VRC&HI-BG).

We investigate two distinct process configurations, both of which incorporate complete HI across the three distillation columns. The vapor outlet of the FAME column undergoes heat exchange with the bottoms of the glycerol column and subsequently the methanol column, serving as the essential heat source for evaporating their respective bottoms. We impose constraints on the temperature differences of the outlet streams of the heat exchangers, stipulating a minimal temperature difference of 10 °C. The differing element between the two configurations lies in the presence or absence of supplementary external heating sources for the reboilers of the methanol and glycerol columns. These configurations are denoted as HI-Cen and HI&Q-Cen, respectively, with the added heating sources indicated by red arrows pointing toward the reboilers (cf. Fig. 1). The optimization variables are highlighted by arrows, wherein $T_{\mathrm{sp,MeOHcol}}$ and $T_{\mathrm{sp,GLYcol}}$ are exclusive to HI&Q-Cen configuration, acting as additional optimization variables. For both configurations, a centralized optimization approach is employed, entailing the resolution of the corresponding optimization problems articulated in Section 3.

2.2 Process configuration with vapor recompression and heat integration

Considering the high computational demands and challenges in achieving convergence when addressing large-scale DO problems, we propose an alternative configuration for HI that allows for the use of a decentralized optimization approach. In El Wajeh et al. (2024), we demonstrated that by introducing the buffer tank, `InterTankOil`, alongside the cooler, CoolerOil, we can fix and thus tear the residual oil recycle, as depicted in Fig. 2. This, in turn, allows for the decoupling of the upstream processes of `InterTankRSR` from its downstream processes. Consequently, we perform HI exclusively for the FAME and glycerol columns while employing VRC for the methanol column (cf. Fig. 2). Our method involves direct VRC for the methanol column, utilizing the vapor leaving from the top of the column. This vapor is compressed, condensed within the reboiler, and partially refluxed back to the column after pressure reduction via a valve. To ensure balanced heat input, particularly due to compressor-generated heat, a trim condenser becomes necessary (Harwardt and Marquardt (2012)).

By leveraging this approach, we can implement two separate decentralized optimizers for the two distinct process parts, as illustrated in Fig. 2. This stands in contrast to

relying on a centralized optimizer, as for the cases of HI-Cen and HI&Q-Cen. These decentralized optimizers are designated as VRC&HI-RSR and VRC&HI-BG, collectively referred to as VRC&HI-Dec for this specific process configuration. This methodology involves tackling two distinct DO problems, encompassing smaller differential-algebraic equation (DAE) systems. Consequently, this approach mitigates non-convergence concerns and reduces overall computational costs.

3. DYNAMIC OPTIMIZATION PROBLEM

In all the process configurations under consideration, our objective is to maximize the operating profit of the process while satisfying all operational constraints within a finite time horizon. Our assessment of operating profit includes the revenue generated by all process products, accounting for all material and energy costs, where electricity prices fluctuate as a time-variant parameter. The optimization variables (cf. Fig. 1) encompass feed flow rates ($\dot{n}_{\mathrm{Oil}}$, $\dot{n}_{\mathrm{MeOH}}$, and $\dot{n}_{\mathrm{Base}}$), the temperature change of the transesterifier jacket fluid ($\Delta T_{\mathrm{Jacket}}$), temperature setpoints for the column reboilers ($T_{\mathrm{sp,MeOHcol}}$, $T_{\mathrm{sp,FAMEcol}}$, and $T_{\mathrm{sp,GLYcol}}$), and outlet flow rates from the transesterifier and intermediate buffer tanks ($\dot{n}_{\mathrm{TransOut}}$, $\dot{n}_{\mathrm{InterTankRSR}}$, $\dot{n}_{\mathrm{InterTankB}}$, and $\dot{n}_{\mathrm{InterTankG}}$). Purity limits for final biodiesel and glycerol products, along with their required production rates, serve as path constraints. Liquid levels within the reactors, decanter, column trays, distillate drums, reboilers, and all buffer tanks are also subject to path constraints. Furthermore, buffer tanks have endpoint constraints, regulating liquid levels and content purity, preventing optimizers from exploiting initial tank conditions, and ensuring convergence to a similar state as the process's initial state. For a comprehensive understanding of optimization problem formulations and mathematical definitions, we direct readers to our prior work (El Wajeh et al. (2024)).

4. SCENARIO AND IMPLEMENTATION

In the simulations of all considered optimization strategies, the demand-response scenario spans a one-day time frame, during which a constant production demand of 20 t/h for biodiesel and 2.12 t/h for glycerol must be met. To capture the electricity price dynamics, we utilize historical data from the German day-ahead spot market for September 3, 2022 (SMARD (2023)), which is depicted in Fig. 3. Raw material and final product prices remain constant throughout. Within the domain of all DO problems, the optimization variables are discretized at uniformly spaced intervals of one hour, while the constraints undergo discretization at 30-minute intervals.

In terms of additional benchmarks, we establish a comparison between the dynamically operated three configurations and their corresponding SS counterparts. Furthermore, we compare these configurations against an optimally flexible operation scenario, similar to the one depicted in Fig. 1, but excluding the incorporation of HI. We refer to this scenario as NoHI-Cen, where we also employ a centralized optimization approach.

Using our open-source optimization framework DyOS (Caspari et al. (2019)), we employ direct single-shooting

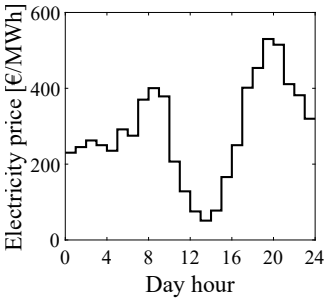

Fig. 3. Electricity prices in the German day-ahead spot market on September 3, 2022 (SMARD (2023)).

(Sargent and Sullivan (1978)) for solving all optimization problems under consideration. The DAE integrator utilized is NIXE (Hannemann et al. (2010)), while SNOPT (Gill et al. (2005)) is employed as the (local) optimization solver. The underlying model comprises 182 differential and 10336 algebraic variables and is developed in Modelica and integrated into DyOS as a Functional Mockup Unit. We configure the DAE integrator tolerances at 10^{-5}, and the solver feasibility and optimality tolerances at 10^{-4}.

5. RESULTS AND DISCUSSION

In order to assess the extent of operational flexibility within the three proposed process configurations for HI, we start by discussing the results pertaining to the production rates of biodiesel and glycerol, in addition to the total power consumption of the process. Following this, we undertake a comparative analysis of their economic performances against the NoHI-Cen configuration, considering energy and material costs, as well as profits. Furthermore, we conduct a parallel evaluation relative to their respective SS operations. Lastly, we evaluate the computational performances, particularly the CPU-time savings arising from implementing the decentralized optimization approach VRC&HI-Dec.

5.1 Production rates and power demand

Comparing the biodiesel production rate results depicted in Fig. 4a with those of the NoHI-Cen configuration, it becomes evident that the three HI configurations exhibit reduced operational flexibility. Specifically, the NoHI-Cen configuration showcases the capacity to operate at notably reduced levels, especially during time intervals between 17.5 and 24. This behavior arises due to the constraints imposed by the HI of process columns, notably the FAME and glycerol columns, which in turn limit the degrees of freedom available for optimization. As opposed to the NoHI-Cen configuration, where the biodiesel production rates can attain these lower limits, the HI configurations display fewer instances of reaching maximal production rates, such as during the periods spanning 5.5 to 7.5.

Analyzing the production profile of the HI-Cen configuration in Fig. 4a, it becomes apparent that biodiesel production flexibility is comparatively diminished in comparison to the HI&Q-Cen and VRC&HI-Dec configurations. This observation underscores the advantages of employing external heating sources to enhance the production flexibility of biodiesel. Moreover, the profile of the VRC&HI-Dec configuration exhibits higher flexibility in contrast to

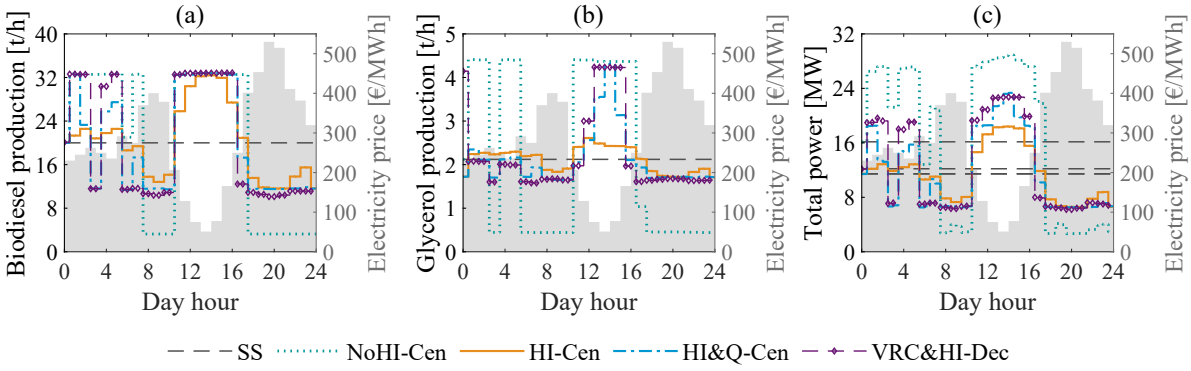

Fig. 4. Production rates and overall power demand results for all examined configurations, both in dynamic operation and their corresponding SS counterparts. (a), (b), and (c) show the production rates of biodiesel and glycerol and the overall power consumption, respectively. SS represents the steady-state operations. The power demand results for steady-state operations in (c) correspond to NoHI-Cen, HI-Cen, and HI&Q-Cen, shown in descending order of values, respectively. The shaded regions within the graphs illustrate the electricity price profile corresponding to the secondary axes.

the HI&Q-Cen configuration. This illustrates that heat-integrating solely the glycerol and FAME columns while simultaneously utilizing an additional heating source, confers enhanced production flexibility compared to the full HI of all three columns.

Examining Fig. 4b, the flexibility in glycerol production is significantly reduced for the HI configurations in comparison to NoHI-Cen. Within the glycerol column, the flow rates are tightly limited to the extent of heat transfer occurring in the column reboiler that engages in thermal exchange with the vapor outlet stream of the FAME column. This interplay imposes limitations, especially evidenced by the incapacity to reduce flow rates beyond specific thresholds, a notable contrast to the NoHI-Cen configuration. Furthermore, the power consumption of the glycerol column during nominal operations is approximately half that of the NoHI-Cen configuration, leading to a decreased necessity for extensive flexibility in glycerol production.

Additionally, the pronounced advantages stemming from the incorporation of supplementary heating sources become clearly apparent. This holds particularly true during the period between 11.5 to 15.5 in Fig. 4b. During this interval, the flexibility in glycerol production rates experiences a significant sudden increase in both the HI&Q-Cen and VRC&HI-Dec configurations. Incorporating the supplementary heating sources facilitates increasing the flow rates within both the methanol and glycerol columns, enabling them to approach higher thresholds. The necessary heating duties for vaporizing these increased flow rates through their respective reboilers are met by the supplementary heating sources. That goes beyond the constraints solely imposed by the extent of heat exchange with the vapor outlet stream of the FAME column, as observed in the HI-Cen configuration.

The examination of total power consumption, as depicted in Fig. 4c across the three HI configurations, stems from the identical analysis applied to biodiesel and glycerol production rates. In general, there is a noticeable reduction in flexibility when compared to the NoHI-Cen configuration. Notably, the enhanced flexibility observed in HI&Q-Cen and VRC&HI-Dec in comparison to HI-Cen aligns with the increased flexibility observed in the production rates. This alignment becomes particularly pronounced during the timeframe from 11.5 to 15.5, wherein the increased glycerol production rates contribute to an additional layer of flexibility.

5.2 Economic evaluation

Table 1 provides an overview of the total profit, energy cost, and material cost associated with each considered HI configuration, compared against those of NoHI-Cen. As anticipated, the incorporation of HI across all configurations yields substantial reductions in energy costs, with VRC&HI-Dec displaying the least pronounced decrease. Noteworthy is that while material costs experience an increase, the overall profits remain superior to those of the NoHI-Cen baseline.

Table 1. Operating profit, energy cost, and material cost for each optimizer. The savings relative to NoHI-Cen are given in parentheses.

	NoHI-Cen	HI-Cen	HI&Q-Cen	VRC&HI-Dec
Energy cost [k€]	80	67 (17 %)	65 (18 %)	68 (14 %)
Material cost [k€]	556	560 (−0.6 %)	558 (−0.2 %)	563 (−1.2 %)
Profit [k€]	679	688 (1.4 %)	692 (2 %)	685 (1 %)

In Table 2, we present a comparative evaluation of profit and cost outcomes for each HI configuration in relation to their corresponding SS operations. Within all HI configurations, the attained savings, though significant, fall short of those realized by NoHI-Cen. This underscores the additional constraints that HI introduces, thereby constricting the available optimization degrees of freedom. In comparison to HI-Cen, both HI&Q-Cen and VRC&HI-Dec yield heightened energy cost savings, emphasizing the elevated flexibility stemming from the incorporation of external heating sources. Furthermore, VRC&HI-Dec surpasses HI&Q-Cen in energy cost savings due to its distinct configuration wherein HI is confined to the FAME and

Table 2. Savings of energy and material costs and increase in profit for each optimizer relative to its corresponding SS operation.

	NoHI-Cen	HI-Cen	HI&Q-Cen	VRC&HI-Dec
Energy cost	29 %	16 %	17 %	19 %
Material cost	1.4 %	0.7 %	1.1 %	0.2 %
Profit	6.1 %	2.4 %	2.9 %	2.7 %

glycerol columns, thus expanding optimization options. Additionally, it is worth highlighting that the increase in total profit for the HI configurations is comparatively more restrained compared to NoHI-Cen.

5.3 Computational performance

In Fig. 5, we provide the CPU times required for solving the DO problems associated with the three HI configurations. As anticipated, the adoption of a decentralized optimization strategy in VRC&HI-Dec yields a notable reduction in CPU time, amounting to approximately threefold savings when compared to HI-Cen or HI&Q-Cen. Additionally, in the process of configuring and scaling the optimization problems for VRC&HI-Dec, a lesser degree of effort was expended, owing to the comparatively smaller DAE systems. This, in turn, led to improved convergence during the problem-solving phase.

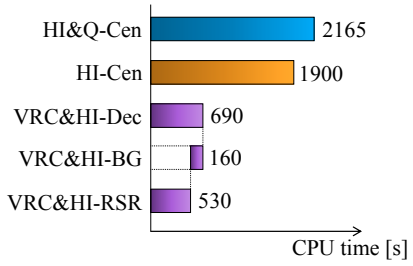

Fig. 5. CPU times for solving the dynamic optimization problems of the considered process configurations.

6. CONCLUSION

While incorporating external heating sources for the reboilers may not be a primary concern when optimizing for steady-state profitability, we demonstrate that this configuration, as applied to biodiesel production, delivers superior results in dynamic operation, especially when considering demand-side management. Furthermore, despite that the configuration employing a decentralized optimization approach involves a lesser extent of heat integration and subsequently fewer energy cost savings, its superior computational performance renders it more suitable for online applications. This is especially relevant for economic nonlinear model predictive control, which will be the focus of our future work. It is worth noting that the results obtained from our investigation in the context of biodiesel production may not necessarily apply to other chemical processes to the same extent. Different processes may encounter limitations due to constraints on educts storage or may have fewer degrees of freedom in optimization. Nevertheless, it is crucial to emphasize that the selection of heat integration process configurations necessitates a departure from conventional process designs, especially when considering dynamic operation applications.

ACKNOWLEDGEMENTS

The authors gratefully acknowledge the financial support of the Kopernikus project SynErgie by the Federal Ministry of Education and Research (BMBF) and the project supervision by the project management organization Projektträger Jülich.

REFERENCES

Barton, J.L. (2020). Electrification of the chemical industry. *Science*, 368(6496), 1181–1182.

Caspari, A., Bremen, A.M., Faust, J., Jung, F., Kappatou, C.D., Sass, S., Vaupel, Y., Hannemann-Tamás, R., Mhamdi, A., and Mitsos, A. (2019). DyOS - A framework for optimization of large-scale differential algebraic equation systems. In *Computer Aided Chemical Engineering : 29 ESCAPE*, volume 46, 619–624. Elsevier.

Cegla, M., Semrau, R., Tamagnini, F., and Engell, S. (2023). Flexible process operation for electrified chemical plants. *Current Opinion in Chemical Engineering*, 39, 100898.

Chen, C. and Yang, A. (2021). Power-to-methanol: The role of process flexibility in the integration of variable renewable energy into chemical production. *Energy Conversion and Management*, 228, 113673.

El Wajeh, M., Mhamdi, A., and Mitsos, A. (2023). Dynamic Modeling and Plantwide Control of a Production Process for Biodiesel and Glycerol. *Industrial & Engineering Chemistry Research*, 62(27), 10559–10576.

El Wajeh, M., Mhamdi, A., and Mitsos, A. (2024). Optimal Design and Flexible Operation of a Fully Electrified Biodiesel Production Process. *Industrial & Engineering Chemistry Research*, 63(3), 1487–1500.

Gill, P.E., Murray, W., and Saunders, M.A. (2005). SNOPT: An SQP algorithm for large-scale constrained optimization. *SIAM Review*, 47(1), 99–131.

Guedes do Nascimento, L., Costa Monteiro, L.P., de Cássia Colman Simões, R., and Prata, D.M. (2023). Eco-efficiency analysis and intensification of the biodiesel production process through vapor recompression strategy. *Energy*, 275, 127479.

Hannemann, R., Marquardt, W., Naumann, U., and Gendler, B. (2010). Discrete first- and second-order adjoints and automatic differentiation for the sensitivity analysis of dynamic models. *Procedia Computer Science*, 1(1), 297–305.

Harwardt, A. and Marquardt, W. (2012). Heat-integrated distillation columns: Vapor recompression or internal heat integration? *AIChE Journal*, 58(12), 3740–3750.

Mitsos, A., Asprion, N., Floudas, C.A., Bortz, M., Baldea, M., Bonvin, D., Caspari, A., and Schäfer, P. (2018). Challenges in process optimization for new feedstocks and energy sources. *Computers & Chemical Engineering*, 113, 209–221.

Sargent, R.W.H. and Sullivan, G.R. (1978). The development of an efficient optimal control package. In J. Stoer (ed.), *Optimization Techniques*, 158–168. Springer Berlin Heidelberg, Berlin, Heidelberg.

SMARD (2023). Market data visuals. `http://www.smard.de`. Accessed: March 22, 2023.